Chemical nature of nitric oxide storage forms in rat vascular tissue

Juan Rodriguez*†, Ronald E. Maloney*, Tienush Rassaf*, Nathan S. Bryan*, and Martin Feelisch*‡

*Department of Molecular and Cellular Physiology, Louisiana State University Health Sciences Center, Shreveport, LA 71130; and †Department of Physics, Centenary College of Louisiana, Shreveport, LA 71134

Edited by Louis J. Ignarro, University of California School of Medicine, Los Angeles, CA, and approved November 14, 2002 (received for review July 31, 2002)

Endothelial NO production results in local formation of adducts that may act as storage forms of NO. Because little is known about their chemical nature, concentrations, and possible role in vascular biology, we sought to characterize those species basally present in rat aorta, using two independent approaches. In the first approach, tissue homogenates were analyzed by using chemiluminescence- and ion-chromatography-based techniques that allow trace-level quantification of NO-related compounds in complex biological matrices. In the second approach, NO stores were characterized by their ability to release NO when illuminated with light and subsequently relax vascular smooth muscle (photorelaxation). The latter included a careful assessment of action spectra for photorelaxation, taking into account the light-scattering properties of the tissue and the storage depletion rates induced by exposure to controlled levels of light. Biochemical analyses revealed that aortic tissues contained 10 ± 1 μM nitrite, 42 ± 7 μM nitrate, 40 ± 6 nM *S*-nitroso, and 33 ± 6 nM *N*-nitroso compounds ($n = 4–8$). The functional data obtained suggest that the NO photolytically released in the tissue originated from species with photophysical properties similar to those reported for low-molecular-weight *S*-nitrosothiols, as well as from nitrite. The relative contribution of these potential NO stores to the extent of photorelaxation was consistent with their concentrations detected biochemically in vascular tissue when their photoactivity was taken into account. We conclude that intravascular nitroso species and nitrite both have the potential to release physiologically relevant quantities of NO independent of enzymatic control by NO synthase.

Much attention has been devoted recently to the role of *S*-nitrosothiols (RSNO) in plasma and circulating erythrocytes, where they are believed to act as a buffer and transport system for NO that is involved in the regulation of vascular tone and blood flow (1–3). The existence of such transporters may have profound implications for the regulation of tissue perfusion, inasmuch as this system appears to operate independently of local enzymatic control via NO synthase. Considerably less attention has been paid to the presence of NO-related products in extraluminal compartments, such as cells of the vascular wall, where they arise as a consequence of endothelial NO production. It is conceivable that such tissue products could also contribute to local blood flow regulation and provide, e.g., additional antiadhesive protection, if bioactivated to regenerate NO. This may be of particular significance under conditions of endothelial dysfunction and in disease states known to be associated with impaired enzymatic NO production. Alternatively, they may represent useful diagnostic markers of nitrosative stress.

First evidence for the existence of stored forms of NO has been derived from experiments on the relaxant effect of light on vascular smooth muscle (4). This phenomenon, known as "photorelaxation," is now believed to arise from the electronic excitation of a preformed store that subsequently releases NO. The earliest attempt at identifying the substance associated with this activity was made by Furchgott *et al.* (5) They determined that the action spectrum for photorelaxation in rabbit aorta peaked near 310 nm, with a shoulder near 350 nm. Because this spectrum appeared partially distorted by a strong feature at 280 nm, which was ascribed to protein absorption, no positive chemical identification could be made. It was noted, however, that on incubation with nitrite, a 355-nm feature dominated the action spectrum (6), providing first evidence for the involvement of a NO-related species in the phenomenon of photorelaxation. Subsequent attempts by other groups to identify the light-sensitive substance responsible for this effect produced inconclusive results. Karlsson *et al.* (7) obtained action spectra for photorelaxation in bovine mesenteric arteries that peaked at ≈360–400 nm. The overlap of the peak with the one reported for soluble guanylate cyclase led the authors to believe that the heme moiety of this enzyme was involved. Another study in rabbit aortae (8) revealed an action spectrum for photorelaxation punctuated by a strong peak near 364 nm and a smaller one near 514 nm, suggesting the existence of two separate chromophores. Other attempts at identifying the nature of these photocleavable NO stores have combined biochemical approaches with UV irradiation, yielding similarly ambiguous results. Some of these studies concluded that intracellular (9, 10) or extracellular (11–14) nitrite may undergo photolysis to NO. Indeed, nitrite ions do undergo NO photolysis, showing a maximum around 354 nm (15). Other studies claimed to have identified RSNOs (16–18) as the chemical species responsible for photorelaxation. However, they possess a UV-absorption band peaking in the 330- to 340-nm range (19, 20), which does not coincide with any of the action spectrum peaks reported in previous studies. In addition to the compounds identified above, others could be added to the list for their well-established ability to undergo UV or near-UV photolytic cleavage to NO. These include *N*-nitroso compounds (RNNO), nitrosylmyoglobin (MbNO), iron–sulfur nitrosyl complexes (such as Roussin's Red Salt; RRS), and dinitrosyl iron complexes, which exhibit absorption maxima at 340–390 (21), 420–422 (22), 360–370 (23), and 310 nm (24), respectively.

It is clear from the above that an unequivocal identification of vascular NO stores has yet to be made. Moreover, nothing is known to date about their concentrations in vascular tissue. Such fundamental information, however, is crucial for the assessment of their significance to vascular biology. The objective of the present study was to uncover the identities and concentrations of NO stores in rat aortic tissue. Using biochemical and optical approaches, we show here that the amounts of nitrite and RSNOs fully account for the photorelaxation in this tissue, with the level of photosensitivity of aortic RSNOs being consistent with those reported for low-molecular-weight compounds *in vitro*. The surprising contribution of the supposedly biologically inactive NO decomposition product, nitrite is attributed to its relatively large concentration compared with the more photoactive RSNOs.

Methods

(*i*) Biochemical Determination of the Tissue Concentrations of Nitrite, Nitrate, and Nitroso Species. Thoracic aortae of male Wistar rats (Harlan Breeders, Indianapolis; 320–420 g) were dissected under

This paper was submitted directly (Track II) to the PNAS office.

Abbreviations: RSNO, *S*-nitrosothiol; GSNO, *S*-nitrosoglutathione; SNOAlb, *S*-nitrosoalbumin; MbNO, nitrosylmyoglobin; RRS, Roussin's Red Salt.

‡To whom correspondence should be addressed. E-mail: mfeeli@lsuhsc.edu.

 www.pnas.org/cgi/doi/10.1073/pnas.0234600100

deep ether anesthesia during retrograde *in situ* perfusion with cold oxygenated Krebs–Henseleit (KH) buffer (pH 7.4) of the following composition (mM): 126.8 NaCl/5.9 KCl/2.5 $CaCl_2$/1.2 $MgCl_2$/1.2 NaH_2PO_4/30 $NaHCO_3$/5 D-glucose/0.001 indomethacin. The aorta was trimmed free of adventitia and fat in cold oxygenated KH buffer, cut into 4- to 5-mm rings, mounted on tungsten wires, and immersed in an organ bath. After 90 min of equilibration under conditions identical to those described in *ii c*, tissues were homogenized (5:1 v/w) in ice-cold *N*-ethylmaleimide/EDTA (10/2 mM)-containing phosphate buffer (50 mM, pH 7.4) and analyzed immediately. In a subset of rats, tissues were processed without prior incubation in the organ bath. Nitroso species in vascular tissue were quantified by a technique that uses reductive denitrosation followed by chemiluminescence detection of NO in the gas phase and which has been described in detail elsewhere (25). Tissues of four additional animals were analyzed for NO-heme species by direct injection of vascular homogenates into an oxidizing solution comprised of 0.05 M ferricyanide in PBS (26). Total amounts of nitrosyl adducts in vascular tissue were calculated by comparison of peak areas of the samples to those of freshly prepared standards. Intracellular nitrite and nitrate concentrations were measured in aliquots of aortic homogenates after methanol precipitation of proteins (1:1 vol/vol) by using a dedicated HPLC system (ENO-20; EiCom, Kyoto). This method is based on the separation of nitrite and nitrate by ion chromatography, followed by on-line reduction of nitrate to nitrite, postcolumn derivatization with the Griess reagent, and detection at 540 nm. The detection limit is 1 nM for either anion at an injection volume of 100 μl. Absolute amounts detected were converted into tissue concentrations, taking into account a volume of 20 μl for the entire aortic segment homogenized (length, ≈3 cm; diameter, 2 mm; thickness, 0.1 mm).

(*ii*) Optical Characterization of NO Stores. ***(a)* In vitro *characterization of action spectra for NO release from potential NO stores.*** GSNO and *S*-nitrosoalbumin (SNOAlb) as representative low- and high-molecular-weight RSNOs, *N*-dimethylnitrosamine as prototypic *N*-nitrosamine, and nitrite (NO_2^-) and nitrate (NO_3^-) were chosen as reference compounds to carry out NO photocleavage experiments. Solutions of these substances were placed inside a temperature-regulated reaction vessel containing phosphate buffer (50 mM, pH 7.40) maintained at 37°C and continuously purged with nitrogen. The NO evolving as a result of photocleavage was swept with the inert carrier gas into the chemiluminescence analyzer (CLD 77AMsp, ECO Physics, Ann Arbor, MI) and quantified in the gas phase after reaction with ozone. An action spectrum for NO release was constructed for each compound by illumination with a tunable light source by using a 75-W xenon lamp filtered with a 8-nm bandpass monochromator (Shimadzu HPLC detector RF-551, flow cell removed) placed at a distance of 4 cm away from the reaction vessel. Solutions containing the potential NO store candidate were illuminated for periods of 1–2 min following a standard protocol of wavelengths that included 310, 320, 330, 340, 350, 360, 380, 400, 420, and 450 nm, applied in random order. Action spectra for NO release were corrected for variations in optical transmission of the reaction vessel and in output intensity of the illumination source, both of which were determined with the aid of a thermopile-based radiometer (detector 70262 and optical power meter 70310, ThermoOriel, Stratford, CT). The transmission of the reaction vessel from the exterior wall of the chamber to its center was estimated from the square root of the transmission across the full width. All wavelength transmission values across the full width of the vessel were determined from the ratio of transmitted to incident intensity and normalized to the corresponding ratio at 340 nm. The wavelength-dependent correction factors for the reaction chamber are listed in Table 2, which is published as supporting information on the PNAS web site, www.pnas.org.

Table 1. Photochemical properties of NO-related substances and aortic tissue stores, in the spectral range of 310–450 nm

Substance	λ_{max}, nm	Ψ_{max}, 10^{-18}·cm^2
GSNO	330–340	2.3
SNOAlb	310	1
DMNA	330–370	0.04
Nitrite	310, 350	0.015
Nitrate	302	<0.00001
DNIC	310	ND
RRS	360–370	5.4
Mb-NO	420–422	0.8
Aorta (untreated)	330–340	4
Aorta (optically depleted)	310, 340–360	<0.06

ND, not determined. DMNA, *N*-dimethylnitrosamine.

(b) Calculation of* in vitro *photoactivity of potential NO stores. The photoactivity of an NO store, denoted here by Ψ, is defined in this study as the rate of photolysis per incident photon per NO store, i.e.,

$$\Psi = \left(\frac{dN}{dt}\right)_{\text{photolysis}} \frac{1}{FN}, \qquad [1]$$

where N is the NO-store concentration, and F is the photon flux. Eq. **1** can be expressed in terms of the extinction coefficient ε and the quantum yield of photolysis φ with the aid of the definition of photolysis quantum yield $(dN/dt)_{\text{photolysis}} = \varphi(dN/dt)_{\text{absorption}}$ and the optical rate equation (27) $(dN/dt)_{\text{absorption}} = -\sigma FN$, where σ is the absorption cross section, and F is the photon flux. From these relations, and the conversion σ (in cm^2) = 1,000 ln(10)ε/N_A (ε in M^{-1}·cm^{-1}), one obtains the formula

$$\Psi = 1000 \ln 10 \varphi\varepsilon/N_A, \qquad [2]$$

which was used in this study to calculate the photoactivity of NO-related species from published ε and φ values. Calculated values of photoactivity at the maximal extinction coefficient ε_{max} for several substances are listed in Table 1, including GSNO, SNOAlb, MbNO, and RRS.

For substances where published values of ε or φ were not available, the photoactivity was estimated experimentally from the photolysis experiments described above. This was achieved by comparing the response $(dN/dt)_{\text{photolysis}}$ obtained with the NO analyzer for a given substance X with that of GSNO, by using the following modified version of Eq. **1**:

$$\Psi_X = \Psi_{\text{GSNO}} \frac{\left(\frac{dN}{dt}\right)_X \int F_{\lambda\,\max X} N_X}{\left(\frac{dN}{dt}\right)_{\text{GSNO}} \int F_{\lambda\,\max \text{GSNO}} N_{\text{GSNO}}}. \qquad [3]$$

Substances included in this group included nitrite, nitrate, and *N*-dimethylnitrosamine. The photoactivity of nitros(yl)ated protein complexes such as SNOAlb and MbNO could not be evaluated by this method, because the release of NO from them may be influenced by subsequent trapping of the radical into hydrophobic pockets within the protein. Such trapping would lead to an underestimation of the true quantum yield of NO photocleavage from the primary binding site in these substances.

(c) Action spectra for photorelaxation in rat aortae. Aortic tissue was obtained from male Wistar rats (220–360 g) and sectioned into 4- to 5-mm rings. The individual rings were mounted between two tungsten rods, placed inside an organ chamber filled with 20 ml of Krebs–Henseleit buffer (pH 7.4, 37°C), and continuously bubbled with oxygen (95% O_2/5% CO_2). Changes in isometric tension were

PHYSIOLOGY

measured by means of force displacement transducers (F30 type 372; Hugo Sachs Electronics, March, Federal Republic of Germany) and documented on a chart recorder (Graphtec Mark VII, WR3310 with Bridge couplers type 570; HSE). Tissues were allowed to equilibrate for 90 min under a resting tension of 2.0 g with complete exchange of the bathing medium every 20 min. After final adjustment of the resting tension, vascular segments were contracted submaximally with 0.2 μM $R(-)$-phenylephrine, and photorelaxation experiments started after contraction had reached a stable level.

Action spectra were obtained from photorelaxation measurements at multiple wavelengths by using the same tunable illumination source used for the photolysis experiments described above shining directly on the organ bath from a distance of 4 cm. The irradiance at the tissues varied from 0.1 to 0.5 mW/cm^2, depending on wavelength. Tissues were illuminated for a period of only 30 s at each wavelength to avoid photodepletion of highly photoactive NO stores. Preliminary investigations revealed that aortic segments were sensitive mostly to wavelengths in the range of 310–360 nm, and no measurable response was observed at wavelengths >500 nm. These data led us to define a standard protocol of wavelengths in the range 310–500 nm. All measurements were performed with dimmed ambient lighting (<15 lux). Our preliminary investigations also indicated that prolonged light exposure resulted in a partial depletion of the relaxation response that occurred rapidly, whereas the remaining response showed no sign of decay. This kinetic behavior suggests the presence of two or more storage forms of NO possessing different photoactivities and possibly different action spectra for NO release. The latter possibility was investigated here with measurements after a 60-min exposure of tissues to 335 nm of light. Action spectra for photorelaxation after optical depletion were obtained with illumination periods of 2 min at multiple wavelengths.

The above action spectra obtained before and after optical depletion were corrected for spectral variations in the output of the light source, transmission of the organ baths, and transmission through the aortic tissue itself. Corrections for spectral variations in light output and organ bath transmission were performed as described in *ii a*. Correction for the internal transmission in the tissue itself required a more elaborate procedure involving the characterization of tissue light scattering and absorption, because these processes affect the photon flux in the interior of the sample by way of attenuation, due to absorption within the sample and reflection losses, and by flux-enhancement due to multiple scattering within the tissue. Both processes are wavelength-dependent. The flux attenuation was estimated to a first approximation as the transmitted flux across the wall into the lumen of the aortic segment. The flux enhancement was determined by estimation of the differential pathlength (28). Both estimates were made with the aid of three types of optical measurements shown in Fig. 1, namely the integrated transmittance (Fig. 1*A*), the integrated reflection (Fig. 1*B*), and the collimated (or unscattered) transmittance (Fig. 1*C*).

The integrated transmittance and reflectance of rat aortic tissue were measured with the aid of a 6-in integrating sphere (Newport, Fountain Valley, CA, 819-IS-6). The system used an illumination source based on a Xenon flash lamp pulsating at a rate of 10 Hz. The light was coupled into a 0.25-m monochromator equipped with a ruled grating (1,200 lines per mm and blazed for 500 nm) and 1-mm slits. Tissue samples consisted of aortic segments measuring 10 mm in length that were cut longitudinally, unfolded, and kept flat between the faces of a 100-μm-pathlength quartz cell (Hellma, Forest Hills, NY, QS 201-2) filled with buffer solution. The light output from the monochromator was collected and focused onto the sample with a quartz lens. For transmittance measurements (see Fig. 1*A*), the tissue sample was positioned at the entrance port of the integrating sphere. The integrated transmitted light collected by the sphere was captured by a photomultiplier tube placed in the sphere wall and connected to a storage oscilloscope (Hewlett–Packard 54616), where the signal was averaged and recorded. The transmission coefficient was determined from the ratio of the above transmission measurement to one performed without tissue. A similar procedure was followed for the reflectance measurements. For the latter, the tissue was positioned at the exit port of the sphere (see Fig. 1*B*) and its signal compared with a 99% reflectance standard.

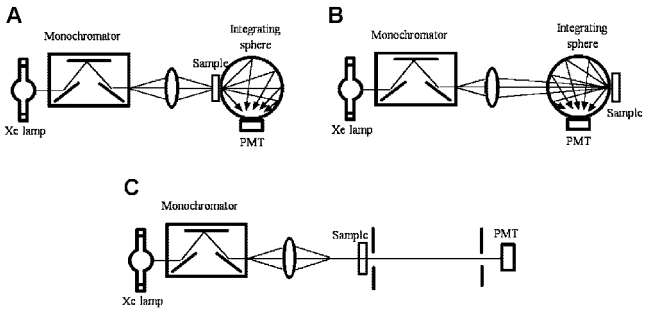

Fig. 1. Diagram of the optical system used for the determination of the optical transmission and the differential pathlength in rat aorta, which were used to compensate photorelaxant responses for internal tissue filtering. Determination of these factors was achieved by measurements of the integrated transmittance (*A*), diffuse reflectance (*B*), and collimated transmittance (*C*) of the sample, and data were processed by using software that simulates the transport of photons via a Monte Carlo technique.

The collimated transmittance was measured by using a separate experimental set-up (see Fig. 1*C*). In this arrangement, the output light from the monochromator was collimated with the aid of two pinholes (3 and 2 mm in diameter) separated by 22 cm, and the sample placed 25 cm before the first. A photomultiplier tube connected directly to the oscilloscope measured the collimated transmission, with and without tissue, and the collimated transmittance was calculated from the ratio of the former to the latter.

The integrating sphere and collimated transmittance measurements were processed with the software package MAGICLIGHT (courtesy of Ilya Yaroslavsky, Palomar Medical Technologies, Lexington, MA). The software is based on a Monte Carlo technique (29) that simulates the transport of photons in a turbid medium and a quasi-Newton inverse solver to generate self-consistent solutions. This program produced estimates of the absorption coefficient as well as the fraction of photons absorbed by the tissue at each wavelength, which were used in the estimation of the tissue differential pathlength. The overall correction for internal transmission in the tissue was obtained by the product of the aortic wall transmission and the differential pathlength.

(d) Calculation of* in situ *photoactivity of NO tissue stores. The photoactivity Ψ of aortic NO stores was assessed *in situ* via the depletion kinetics they exhibit when exposed to a continuous light flux F. A kinetic model of photodepletion was obtained from integration of Eq. **1**, which suggested a solution of the form

$$N = N_0 e^{-\Psi F t}, \qquad [4]$$

where N_0 is the initial concentration of stores in the tissue. Hence, all photodepletion kinetics were curve-fitted to Eq. **4** to obtain a numerical estimate of the combined factors ΨF. The photon flux F within the tissues was then determined from the flux measurement before the surface of the organ baths with a thermopile-based radiometer and corrected for the coupling efficiency into the tissues due to light divergence through the cell and absorption/scattering effects within the tissues as described in *ii c*. Depletion exposures were carried out for periods of 60 min at 335 nm, using the same tunable arrangement as described above.

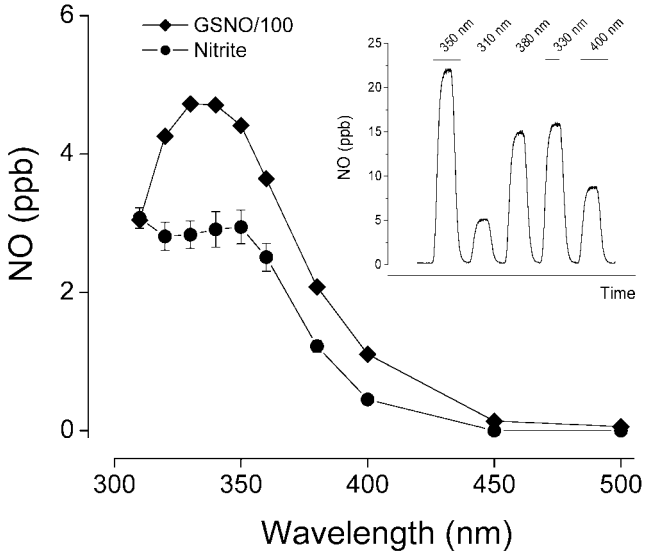

Fig. 2. Action spectra for NO release from GSNO and nitrite in 50 mM phosphate buffer, pH 7.4 and 37°C. The photocleaved NO was purged from the reaction vessel with nitrogen and quantified by gas phase chemiluminescence. Data are the means ± SEM of three individual experiments, with error bars being within symbols in the GSNO spectrum. (*Inset*) Typical tracing obtained with 10 μM GSNO and brief exposures to light of varying wavelengths.

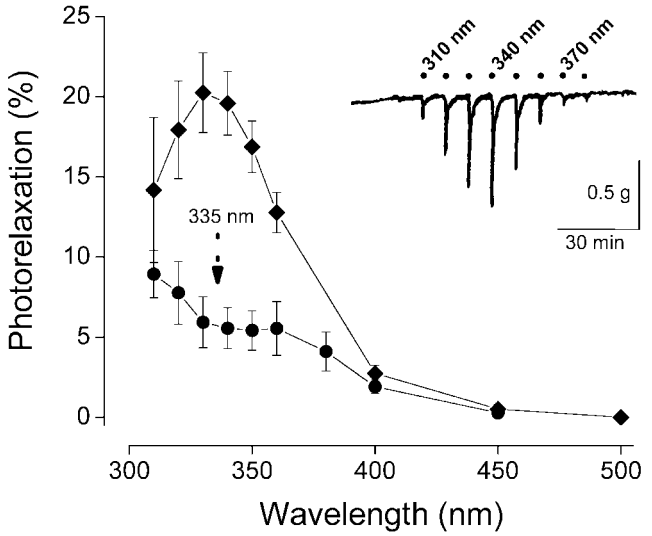

Fig. 3. (*Inset*) Typical ''photorelaxation fingerprint'' responses obtained in precontracted rat aortic rings exposed to brief challenges with light of varying wavelengths. The average action spectra derived from such tracings are shown, following corrections for the wavelength dependence of the intensity of the light source, the transmission of the organ bath, and the internal filtering within the tissue. The percent photorelaxation refers to percent change from contractile tone before illumination. The upper curve represents the average spectrum of 67 rings from 23 animals obtained with 30-s exposures at each wavelength (means ± SEM). The lower curve represents the average action spectrum of 12 rings from seven animals obtained after 60-min exposure to light at 335 nm (0.3 mW/cm^2 irradiance).

Results

(*i*) Biochemical Quantification of Nitrite, Nitrate, and Nitroso Content of Vascular Tissue. The major NO-related species in rat aortic tissue were found to be the end-products of oxidative NO decomposition, nitrite and nitrate. Assuming a homogenous distribution throughout endothelium and smooth muscle, their average tissue concentration corresponded to 10 ± 1 μM nitrite and 42 ± 7 μM nitrate (n = 8). *S*-nitroso and *N*-nitroso compounds were found to be present in roughly equimolar amounts (40 ± 6 nM RSNOs, 33 ± 6 nM RNNOs; n = 4). No *O*-nitroso or heme nitrosyl compounds were detected, suggesting that these species are either not formed at all or in quantitatively negligible amounts. Tissue that was not subjected to the equilibration procedure in the organ bath had very similar nitrite/nitrate levels, but ≈3-fold higher levels of nitroso species (data not shown).

(*ii*) Optical Characterization of NO Stores. ***(a)* In vitro *characterization of action spectra for NO release from potential NO stores.*** Action spectra for NO release from a series of representative candidate NO stores were constructed by using discrete wavelengths of light as outlined in *Methods*. A representative tracing of GSNO photolysis is shown in Fig. 2 *Inset*. The corrected action spectra for NO release from GSNO and *N*-dimethylnitrosamine were found to closely match the absorption spectra of these compounds, peaking in the 330- to 340-nm range. The corresponding photolysis spectra for nitrite and SNOAlb were markedly broader compared with their UV absorption spectra. Nitrite photolysis peaked at 350 nm with another maximum at or below 310 nm, whereas SNOAlb exhibited gradually rising levels of NO release as the wavelength is decreased. No detectable NO release was obtained with exposure of nitrate to light in the 310- to 400-nm range. The wavelength maxima of these action spectra are listed in Table 1.

The spectral profiles of GSNO and nitrite photolysis were found to be concentration-independent. In the case of nitrite, the efficacy of photolysis (photoactivity) was concentration-dependent, following a power dependence of ≈0.58. In contrast, the photoactivity of GSNO scaled linearly with concentration. Fig. 2 depicts the action spectra for NO release from GSNO and nitrite. Both spectra were obtained at concentrations similar to those measured for nitrite in aortic tissue (10 μM) with the GSNO spectrum adjusted by a factor of 100 to bring both spectra onto the same scale and to reflect more closely the biochemically determined concentration ratio of RSNO/nitrite in the tissue.

(b) Calculation of* in vitro *photoactivity of potential NO stores. Photoactivity values for GSNO, SNOAlb, RRS, and MbNO were calculated by using the formula shown in Eq. **2** and reported values of ε_{max} and φ for these compounds, (19, 22, 23, 30), whereas corresponding values for nitrite, nitrate, and *N*-dimethylnitrosamine were determined from data of *in vitro* photolysis experiments by using Eq. **3**. The results of our calculations, summarized in Table 1, place RRS as the most photoactive substance (5.4×10^{-18}·cm^2), followed by GSNO (2.3×10^{-18}·cm^2), SNOAlb (1×10^{-18}·cm^2), and MbNO (0.8×10^{-18}·cm^2). The surprisingly low photoactivity of MbNO is due to efficient (99.85%) geminate recombination of the NO moiety with the heme.

The photoactivity of *N*-dimethylnitrosamine, nitrite, and nitrate, which were found with the aid of Eq. **3**, yielded values of 4×10^{-20}, 1.5×10^{-20}, and $<10^{-23}$·cm^2, respectively. In the case of nitrite, as stated above, the photoactivity reported was found to be concentration-dependent, following a power dependence of ≈0.58. The value reported here for nitrite was obtained at a concentration similar to the one assayed for rat aortic tissue (10 μM). Nitrate photolysis yielded no detectable NO, placing the photoactivity of this substance at a level $<10^{-23}$·cm^2.

(c) Action spectra for photorelaxation in rat aortae. The vascular dilatory response to short-lasting monochromatic exposures at various wavelengths is shown in Fig. 3 *Inset*. The onset of relaxation typically occurred within a few seconds and reached its maximum within 30 s. A total of 67 such tracings obtained with separate aortic segments from 23 animals were averaged and corrected for the spectral distortions by using the correction factors listed in Table 2. In general, the spectral profiles were remarkably consistent in all tissue segments examined, but their overall amplitude varied significantly

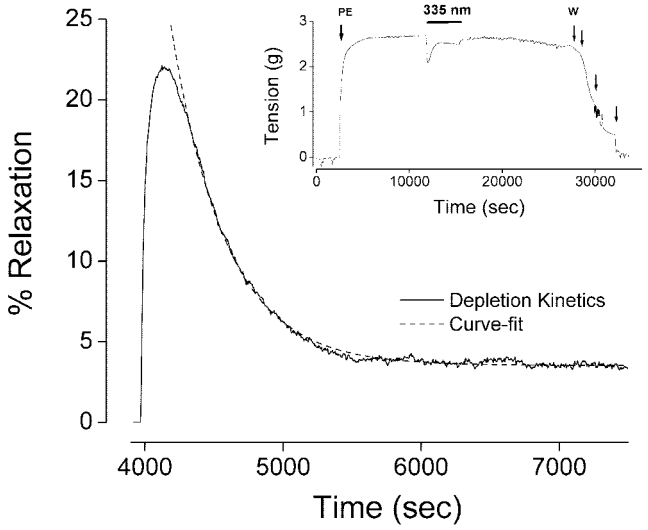

Fig. 4. (*Inset*) Representative tracing of a precontracted rat aortic segment that has been exposed for 60 min to 335-nm light at an irradiance of 0.3 mW/cm^2 (PE, phenylephrine; W, washout). The depletion kinetics of the photorelaxant response observed during the continuous light exposure is magnified and represented as percent relaxation in the main panel (solid curve). The dashed curve represents a curve-fit to a theoretical optical depletion model (Eq. **4**).

between individual animals and along the aortic tree. Typically, relaxations were more pronounced in segments of or near the aortic arch and weaker in the more distal parts. Importantly, the amplitude of the responses exhibited a significant reduction with increasing animal age (not shown). The action spectrum for photorelaxation obtained after averaging is represented by the upper curve in Fig. 3. The spectrum is characterized by a band peaking in the 330- to 340-nm range. After a 60-min exposure to monochromatic light at 335 nm, intended to deplete the above photoactive store, the action spectrum for photorelaxation exhibited a spectral and amplitudinal transformation, resulting in a multifeatured spectrum that peaks around 340–360 nm and at or below 310 nm (see Fig. 3, lower curve). The wavelength maxima of the action spectra for photorelaxation, before and after optical depletion, are tabulated in Table 1.

(d) Calculation of photoactivity of NO stores in rat aortae. With the onset of illumination at 335 nm, a transient vasodilatory response was produced that decayed within a few minutes to a steady-state response of much lower amplitude (Fig. 4). The vasodilatory response decayed exponentially, as predicted by Eq. **4** and demonstrated by the near-perfect superimposition of the curve-fit to this equation (see Fig. 4). Curve-fits were obtained from 10 individual depletion tracings by using paired segments of 5 animals at 335 nm to determine the value for the factor ΨF. An average value of 0.0018 ± 0.0002 sec^{-1} was obtained for ΨF at an estimated irradiance of 0.3 mW/cm^2 (5×10^{14} photons·sec^{-1}·cm^{-2}), from which a photoactivity Ψ of 4×10^{-18}·cm^2 was obtained for the NO-store peaking in the 330- to 340-nm range (Table 1).

After depletion of the above NO store, the photorelaxant response dropped to a lower but sustained level (Fig. 4 *Inset*). This phenomenon is presumably due to the presence of a highly abundant but poorly photoactive NO store. The lack of observable depletion of this second NO store (even with illumination periods exceeding 2 h) prevented us from calculating its photoactivity. Nevertheless, we were able to estimate a limiting value for the photoactivity with the recognition that the lack of observed depletion implies the depletion time for this species must be at least one order of magnitude greater than the exposure time of 1 h used in our experiments. This indicates that the factor $(\Psi F)^{-1}$ must be >36,000 sec, or that ΨF is <0.000028 sec^{-1} at an irradiance of 0.3 mW/cm^2, leading to an upper-bound value of 6×10^{-20}·cm^2 for the photoactivity of the second species (Table 1).

Discussion

The present investigation took advantage of two analytical techniques recently developed in our laboratories to identify and quantify NO stores in vascular tissue. The first technique is a biochemical method capable of assaying vascular tissue homogenates for trace levels of NO-related products, including nitrite, *S*-nitroso, and other nitroso species, which was complemented by an ion-chromatographic method for simultaneous quantification of nitrite and nitrate. The second technique used for the identification of NO-related substances is based on their ability to undergo photolytic cleavage to NO, resulting in a functional vasodilator response. Identification of compounds was achieved through spectral analysis and quantitative assessment of their photosensitivity. Particular attention was given in this study to minimizing artifacts that often challenge UV spectroscopy, including wavelength-dependent changes in intensity of the illumination source, the transparency of the organ chambers used, and internal filtering within tissues. Correction for the latter was possible by advances made during the last decade in the area of tissue spectroscopy, which allowed us to account fully for scattering and absorption effects that take place inside the highly turbid vascular medium. The photoactivity of NO-related products was quantified by their ability to capture an incident photon (i.e., the extinction coefficient) and the probability that the absorbed photon will cleave NO off the substance (i.e., the photolysis quantum yield). The photoactivity so defined is expected to differ among different NO-containing substances, depending on which type of atom NO is bound to and on caging effects at the binding site, and was therefore exploited to further pinpoint the identity of these substances.

Our biochemical studies revealed that rat vascular tissue contains four different products of oxidative and nitrosative NO metabolism, namely nitrite, nitrate, RSNOs, and RNNOs. Of those, RSNOs appeared by far to have the highest photoactivity *in vitro*, followed an order of magnitude lower by RNNOs, and another order of magnitude lower by nitrite. No appreciable NO release was observed from nitrate even at high concentrations. Importantly, our determination of the action spectra for NO release from different RSNOs yielded clearly distinct spectral profiles values for seemingly similar compounds.

Our optical studies in rat aortae clearly revealed the existence of two types of NO-related photoactive substances. This was evidenced by the biphasic nature of the depletion kinetics and the distinctive action spectra for photorelaxation obtained during both phases. The action spectrum and depletion kinetics obtained during the first phase is characterized by a distinct peak at 330–340 nm, and a high photoactivity comparable to those obtained for RSNOs and RRS. Both photolysis properties are consistent with those obtained for GSNO (see Table 1). The identification of this NO store as a GSNO-like compound is in line with recent work by Megson *et al.* (16), who demonstrated that the extent of photorelaxation of the depletable store in rat vascular tissue is modulated by the tissue level of glutathione. The action spectrum for photorelaxation obtained after depletion of the GSNO-like store displayed a broader spectrum that resembled the nitrite action spectrum for NO release. The low photoactivity of this aortic substance was also consistent with that of nitrite (see Table 1).

One of the most striking results of the present study is the close match in the amplitudes of the action spectra for NO release (Fig. 2) and those of the action spectra for photorelaxation (Fig. 3). In Fig. 2, it was necessary to reduce the GSNO values by two orders of magnitude relative to those of nitrite to bring them to the same plotting scale. This scale reduction was necessary due to the low photoactivity of nitrite, which is two orders of magnitude lower than that of GSNO. In Fig. 3, the action spectra for photorelaxation were found to have amplitudes of compa-

rable magnitude, just when our biochemical assay indicates that the concentration of the second NO store (presumably nitrite) was two orders of magnitude larger than that of the first NO store (presumably a GSNO-like substance). The consistency between the biochemical, photolytical, and functional results further argue in favor of a GSNO-like substance and nitrite as the NO stores that dominate the action spectra for photorelaxation.

The identification of two major photoactive NO stores made in the present study may help us understand why previous studies reached different conclusions regarding the nature of the photoactive material. For instance, Furchgott *et al*.'s (5) action spectrum for photorelaxation in rabbit vascular tissue has a strong resemblance to the one we obtained after depletion. This might indicate that the photorelaxation observed originally in rabbit aorta was largely due to nitrite rather than *S*-nitroso substances, as we have observed in rat vascular tissue. The distinction could be indicative of differences in NO-store composition among species and perhaps could be of nutritional origin (herbivores vs. omnivores). Interestingly, when Furchgott (6) incubated his tissues with nitrite, the action spectrum for photorelaxation was significantly enhanced at 355 nm. He later demonstrated that nitrite photolysis released a potent vasodilator, and thus attributed the earlier potentiation of the photorelaxation action spectrum to NO liberation from nitrite photolysis (31). Although the present work clearly confirms that nitrite photolysis releases NO, its action spectrum for NO release does not exhibit a distinct peak at 355 nm. The potentiation obtained with nitrite incubation might therefore rather have been the result of a nitrite-mediated nitrosation of vascular thiols, giving rise to RSNO formation.

Two important points demonstrated in the present study are that compounding spectral artifacts can mask the true identity of photoactive substances in tissues, and that spectral corrections play a key role in uncovering them. According to the correction factors we obtained, all spectral artifacts considered here lead to an underestimation of functional responses elicited by shorter wavelengths of light. In particular, our results showed that tissue internal absorption can lead to significant spectral alterations even in only 100-μm-thick tissues, such as rat aorta. Therefore, the peaks reported by Furchgott (6) at 355 nm and Chaudhry *et al.* (8) at 364 nm, which were obtained in rabbit aorta, a considerably thicker tissue, would likely be manifested at significantly shorter wavelengths if tissue spectral corrections had been implemented. The importance of correcting for UV transmission of the organ bath material was also demonstrated here. This factor is likely to affect the outcome of experiments conducted in the absence of UV-transparent organ baths and may have contributed to further spectral shifting in the previous studies by Karlsson *et al*. (7) and Chaudhry *et al.* (8).

Collectively, the present study provides, to our knowledge, the first unequivocal identification and quantitative assessment of NO stores in vascular tissue. Whereas our functional data clearly demonstrate that these NO stores have the capacity to modulate blood vessel tone, a question that remains unanswered is whether these stores can be bioactivated *in vivo* to the extent they were optically. Earlier *in vitro* studies have demonstrated that RSNOs decompose with the release of NO by heat, light, and interaction with metals, thiols, and ascorbate (32), whereas tissue acidification [e.g., during hypoxia (33)] and enzymatic reduction by xanthine oxidoreductase (34) have been implicated in NO formation from nitrite. Little information is available, however, as to which of these mechanisms might be involved in the bioactivation of NO stores *in vivo*. Besides these mechanistic considerations probably the most crucial question to address in future studies is that of the potential biological significance of NO stores. The undeniable presence of vascular NO stores under basal conditions suggest that they either represent markers of local nitrosative events or serve a physiological function yet to be unraveled. NO stores may not be unique to vascular tissue but exist in other organs and serve other functions. The use of light may be key to elucidating these potential new NO-related pathways in health and disease.

We thank M. Schmidt for expert technical assistance. This work was supported by funds from the Feist Endowment, the Edward P. Stiles Trust Fund, National Institutes of Health Grant HL69029-01 (to M.F.), and a fellowship from the Deutsche Forschungsgemeinschaft (RA-969 1/1 to T.R.).

1. Stamler, J. S., Jaraki, O., Osborne, J., Simon, D. I., Keaney, J., Vita, J., Singel, D., Valeri, C. R. & Loscalzo, J. (1992) *Proc. Natl. Acad. Sci. USA.* **89,** 7674–7677.
2. Minamiyama, Y., Takemura, S. & Inoue, M. (1996) *Biochem. Biophys. Res. Commun.* **225,** 112–115.
3. Jia, L., Bonaventura, C., Bonaventura, J. & Stamler, J. S. (1996) *Nature* **380,** 221–226.
4. Furchgott, R. F., Sleaton, W., Jr., McCaman, M. W. & Elchleff, J. (1955) *J. Pharmacol. Exp. Ther.* **113,** 22–23.
5. Furchgott, R. F., Ehrreich, S. J. & Grennblatt, E. (1961) *J. Gen. Physiol.* **44,** 499–519.
6. Furchgott, R. F. (1971) in *Physiology and Pharmacology of Vascular Neuroeffector Systems*, eds. Bevan, J. A., Furchgott, R. F., Maxwell, R. A. & Somlyo, A. P. (Karger, Basel), pp. 247–282.
7. Karlsson, J. O., Axelsson, K. L., Elwing, H. & Andersson, R. G. (1986) *Cyclic Nucleotide Protein Phosphor. Res.* **11,** 155–166.
8. Chaudhry, H., Lynch, M., Schomaker, K., Birngruber, R., Gregory, K. & Kochevar, I. (1993) *Photochem. Photobiol.* **58,** 661–669.
9. Kubaszewski, E., Peters, A., McClain, S., Bohr, D. & Malinski, T. (1994) *Biochem. Biophys. Res. Commun.* **200,** 213–218.
10. Büyükafsar, K., Demirel-Yilmaz, E., Göçmen, C. & Dikmen, A. (1999) *J. Pharmacol. Exp. Ther.* **290,** 768–773.
11. Trivedi, H. D., Kelkar, V. V., Jindal, M. N. & Dave, K. C. (1978) *Ind. J. Physiol. Pharmacol.* **22,** 136–141.
12. Dave, K. C., Jindal, M. N., Kelkar, V. V. & Trivedi, H. D. (1979) *Br. J. Pharmacol.* **66,** 197–201.
13. Wigilius, I. M., Axelsson, K. L., Andersson, R. G., Karlsson, J. O. & Odman, S. (1990) *Biochem. Biophys. Res. Commun.* **169,** 129–135.
14. Matsunaga, K. & Furchgott, R. F. (1991) *J. Pharmacol. Exp. Ther.* **259,** 1140–1146.
15. Jankowsky, J. J., Keiber, D. J. & Mopper, K. (1999) *Photochem. Photobiol.* **70,** 319–328.
16. Megson, I. L., Holmes, S. A., Magid, K. S., Pritchard, R. J. & Flitney, F. W. (2000) *Br. J. Pharmacol.* **130,** 1575–1580.
17. Lovren, F. & Triggle, C. R. (1998) *Eur. J. Pharmacol.* **347,** 215–221.
18. Venturini, C. M., Palmer, R. M. & Moncada, S. (1993) *J. Pharmacol. Exp. Ther.* **266,** 1497–1500.
19. Wood, P. D., Mutus, B. & Redmond, R. W. (1996) *Photochem. Photobiol* **64,** 518–524.
20. Zhang, Y. Y., Xu, A. M., Nomen, M., Walsh, M., Keaney, J. F., Jr., & Loscalzo, J. (1996) *J. Biol. Chem.* **271,** 14271–14279.
21. Rao, C. N. R. & Bhaskar, K. R. (1981) in *The Chemistry of the Nitro and Nitroso Groups*, ed. Feuer, H. (Krieger, Hunington, NY), pp. 153–154.
22. Kharitonov, V. G., Bonaventura, J. & Sharma, V. S. (1996) in *Methods in Nitric Oxide Research*, eds. Feelisch, M. & Stamler, J. S. (Wiley, Chichester, U.K.), pp. 39–45.
23. Bourassa, J., DeGraff, W., Kudo, S., Wink, D. A., Mitchell, J. B. & Ford, P. C. (1997) *J. Am. Chem. Soc.* **119,** 2853–2860.
24. Lobysheva, I. I., Serezhenkov, V. A. & Vanin, A. F. (1999) *Biochemistry (Moscow)* **64,** 153–158.
25. Feelisch, M., Rassaf, T., Mnaimneh, S., Singh, N., Bryan, N., Jourd'heuil, D. & Kelm, M. (2002) *FASEB J.* **16,** 1775–1785.
26. Gladwin, M. T., Wang, X., Reiter, C. D., Yang, B. K., Vivas, E. X., Bonaventura, C. & Schechter, A. N. (2002) *J. Biol. Chem.* **277,** 27818–27828.
27. Svelto, O. (1989) *Principles of Lasers* (Plenum, New York), 3rd Ed., p. 3.
28. Wray, S., Cope, M., Delpy, D. T., Wyatt, J. S. & Reynolds, E. O. R. (1988) *Biochem. Biophys. Acta* **933,** 184–192.
29. Yaroslavsky, I. V., Yaroslavsky, A. N., Goldback, T. & Schwarzmaier, H.-J. (1996) *Appl. Opt.* **36,** 6797–6809.
30. Rohlfs, R. J., Olson, J. S. & Gibson, Q. H. (1988) *J. Biol. Chem.* **263,** 1803–1813.
31. Matsunaga, K. & Furchgott, R. F. (1988) *J. Pharmacol. Exp. Ther.* **248,** 687–695.
32. Hogg, N. (2002) *Annu. Rev. Pharmacol. Toxicol.* **42,** 585–600.
33. Zweier, J. L., Wang P., Samouilov, A. & Kuppusamy, P. (1995) *Nat. Med.* **1,** 804–808.
34. Godber, B. L., Doel, J. J., Sapkota, G. P., Blake, D. R., Stevens, C. R., Eisenthal, R. & Harrison, R. (2000) *J. Biol. Chem.* **275,** 7757–7763.